

**Charged droplets-driven fast formation of nickel-iron  
(oxy)hydroxide with rich oxygen defects for boosting overall  
water splitting**

Jianing Dong, Yanjie Wang, Qiaorong Jiang, Zi-Ang Nan, Feng Ru Fan\*, Zhong-Qun  
Tian

<sup>a</sup> State Key Laboratory of Physical Chemistry of Solid Surfaces, Collaborative Innovation Center of Chemistry for Energy Materials (*iChEM*), Tan Kah Kee Innovation Laboratory, College of Chemistry and Chemical Engineering, Xiamen University, Xiamen 361005, China.

\*Corresponding author. E-mail: Feng Ru Fan: [frfan@xmu.edu.cn](mailto:frfan@xmu.edu.cn)

## Table of Contents

<b>Experimental Procedures .....</b>	<b>3</b>
<b>Computational Method.....</b>	<b>5</b>
<b>Supporting Figures and Tables .....</b>	<b>6</b>
<b>Figure S1.....</b>	<b>6</b>
<b>Figure S2.....</b>	<b>7</b>
<b>Figure S3.....</b>	<b>8</b>
<b>Figure S4.....</b>	<b>8</b>
<b>Figure S5.....</b>	<b>9</b>
<b>Figure S6.....</b>	<b>9</b>
<b>Figure S7.....</b>	<b>9</b>
<b>Figure S8.....</b>	<b>10</b>
<b>Figure S9.....</b>	<b>11</b>
<b>Figure S10.....</b>	<b>12</b>
<b>Figure S11.....</b>	<b>13</b>
<b>Table S1.....</b>	<b>13</b>
<b>Table S2.....</b>	<b>14</b>
<b>Table S3.....</b>	<b>15</b>
<b>Table S4.....</b>	<b>16</b>
<b>Table S5.....</b>	<b>17</b>
<b>References .....</b>	<b>177</b>

## Experimental Procedures

***Synthesis of E-NiFeOOH by electrospray ionization:*** Firstly, nickel foam is cleaned by ultrasonic in acetone, hydrochloric acid (3 M) and DI water for 10 min to remove nickel oxide layer and containments, respectively and dried under ambient condition. Then, 0.1 M  $\text{FeCl}_3 \cdot 6\text{H}_2\text{O}$  was dissolved in DI water as a precursor. Then this solution was injected into a fused silica capillary (50  $\mu\text{m}$  inner diameter and 150  $\mu\text{m}$  outer diameter) by a 500  $\mu\text{L}$  syringe (Hamilton) and a syringe pump (Harvard Apparatus) at a rate of 10  $\mu\text{L}/\text{min}$  for 20, 30, 40, 60 min (named as E-NiFeOOH-x min, x represents the electrospray time). The  $8.5 \pm 0.5$  kV is applied between the needle and the glass on the lifts as a receiver which 1 x 1  $\text{cm}^2$  nickel foam placed on with a distance of  $4 \pm 0.3$  cm to form a multi-jet mode to ensure the uniform distribution of charged droplets. During this spraying process, the charged microdroplets diminish in size by a series of solvent evaporation and coulomb fission. The smaller the droplet, the faster the reaction will be accelerated. Thousands of small droplets promote the entire reaction at the confined and charged solid-liquid interface. The electrodes were also rinsed with DI water after the reaction.

***Synthesis of I-NiFeOOH by corrosion engineering:*** The fabrication of NiFeOOH by corrosion engineering only needs to immerse 1 x 1  $\text{cm}^2$  Ni foam into 1.5 mL (0.1 M)  $\text{FeCl}_3 \cdot 6\text{H}_2\text{O}$  (named as I-NiFeOOH) for the same time compared with E-NiFeOOH. It is worth noting that the E-NiFeOOH and I-NiFeOOH were washed several times with DI water to end the spontaneous redox reaction on the surface.

***Synthesis of Pt/C/NF and RuO<sub>2</sub>/NF:*** Pt/C and RuO<sub>2</sub> catalysts are loaded on the Ni foams to fabricate Pt/C/NF and RuO<sub>2</sub>/NF. Briefly, a homogenous ink was obtained by dispersing the commercial 7 mg Pt/C or RuO<sub>2</sub> catalysts in the mixture of 200  $\mu\text{L}$  water and 5  $\mu\text{L}$  Nafion by ultrasonic treatment. And then, all the ink was dropped on the Ni

foam to ensure that the loading mass of Pt/C and RuO<sub>2</sub> were both 2.5 mg/cm<sup>2</sup>.

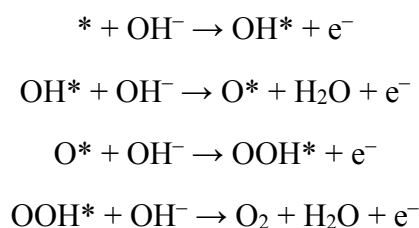
**Material Characterization:** The morphology of NiFeOOH samples was observed using field emission scanning electron microscopy (FE-SEM, Hitachi S-4800, Zeiss-Gmini500) and transmission electron microscopy (TEM, FEI Tecnai F-20 operated at 200 kV). In addition, the high-resolution transmission electron microscope (HRTEM) equipped with energy dispersive X-ray (EDX) spectroscopic analysis (TEM, FEI Tecnai F-20 operated at 200 kV) was employed to give more detailed morphologies. The valence state, surface chemical state, and compositions were explored by X-ray photoelectron spectroscopy (XPS, Thermo Fisher Scientific K-Alpha). XRD patterns were analyzed on an X-ray diffractometer (Rigaku, RINT2500) with a Cu K $\alpha$  radiation source. EPR measurement was done by Bruker EMX-10/12 under 100 K conditions.

**Electrocatalytic Performance Characterization:** The overall water splitting measurements were performed through an electrochemical work station (CHI 660E, Shanghai Chenhua) with a typical three-electrode system: different NiFeOOH samples as work electrodes, graphite rod as a counter electrode and mercury oxide (Hg/HgO) as a reference electrode, 1 M KOH solution as alkaline electrolyte. The HER and OER polarization curves were measured at a scan rate of 5 mV/s. All potentials reported were calibrated to the reversible hydrogen electrode (RHE) by  $E_{RHE} = E_{SCE} + 0.098 \text{ V} + 0.059 \times \text{pH}$ , and all LSV curves were corrected for an ohmic drop (85%) to evaluate the true activity of the electrocatalysts. The electrochemical impedance spectroscopy was obtained in a 1 M KOH solution at 0.1 V from  $10^5 - 10^{-1}$  Hz with an AC voltage amplitude of 5 mV to measure the system resistance. The electrochemical surface area (ECSA) of different samples were gauged by the  $C_{dl}$ , and CV with a different scan rate (20 mV/s, 20 mV/s, 40 mV/s, 80 mV/s, 160 mV/s) was employed to calculate the values of  $C_{dl}$ . The ECSA-normalized LSV curves are calculated by  $ECSA = C_{dl}/C_s$ . A specific capacitance ( $C_s$ ) value  $C_s = 0.040 \text{ mF/cm}^2$ . Moreover, all the presented curves were in their steady-state after several cycles.

## Computational Method

Spin-polarized density functional theory (DFT) calculations were conducted by Vienna Ab-initio Simulation Package (VASP)<sup>[1,2]</sup>, using the projected augmented wave (PAW)<sup>[3]</sup> method. The Perdew-Burke-Ernzerhof (PBE) functional was used to treat the exchange-correlation interaction<sup>[4]</sup>. The Grimme's D3-type of the semiempirical approach was applied to account for the dispersion interaction<sup>[5]</sup>. The Hubbard-U correction method (DFT + U) was adopted for accurately describing Ni/Fe 3d orbitals with U set to 4.0/6.4 eV. The cut-off energy was set to be 450 eV and the convergence threshold was set to  $10^{-4}$  and 0.02 eV/Å for energy and force, respectively. The NiFe-LDH was modelled by a  $3 \times 3$  slab and a  $\sim 15$  Å vacuum layer was applied to prevent the interaction between periodical images. For the NiFe-LDH surface model, 1/4 Ni sites on surface were replaced with Fe atoms.

In the alkaline conditions, the OER involves a four proton-coupled electron transfer (PCET) process, which can be expressed as follows



where \* donates the active site, and OH\*, O\* and OOH\* are OER intermediates. Based on the computational hydrogen electrode (CHE) model [6], the Gibbs free energies for all intermediates during OER were calculated via the equation

$$\Delta G = \Delta E + \Delta E_{\text{ZPE}} - T\Delta S - neU$$

where  $\Delta E$  is the adsorption energy of the adsorbed intermediates, and  $\Delta E_{\text{ZPE}}$  and  $\Delta S$  are the difference in the zero-point energy and the change in entropy before and after adsorption, respectively.  $U$  is the applied potential.

According to the definition, the theoretical overpotential ( $\eta$ ) is defined as

$$\eta = \max(\Delta G)/e - 1.23 \text{ V}$$

## Supporting Figures and Tables

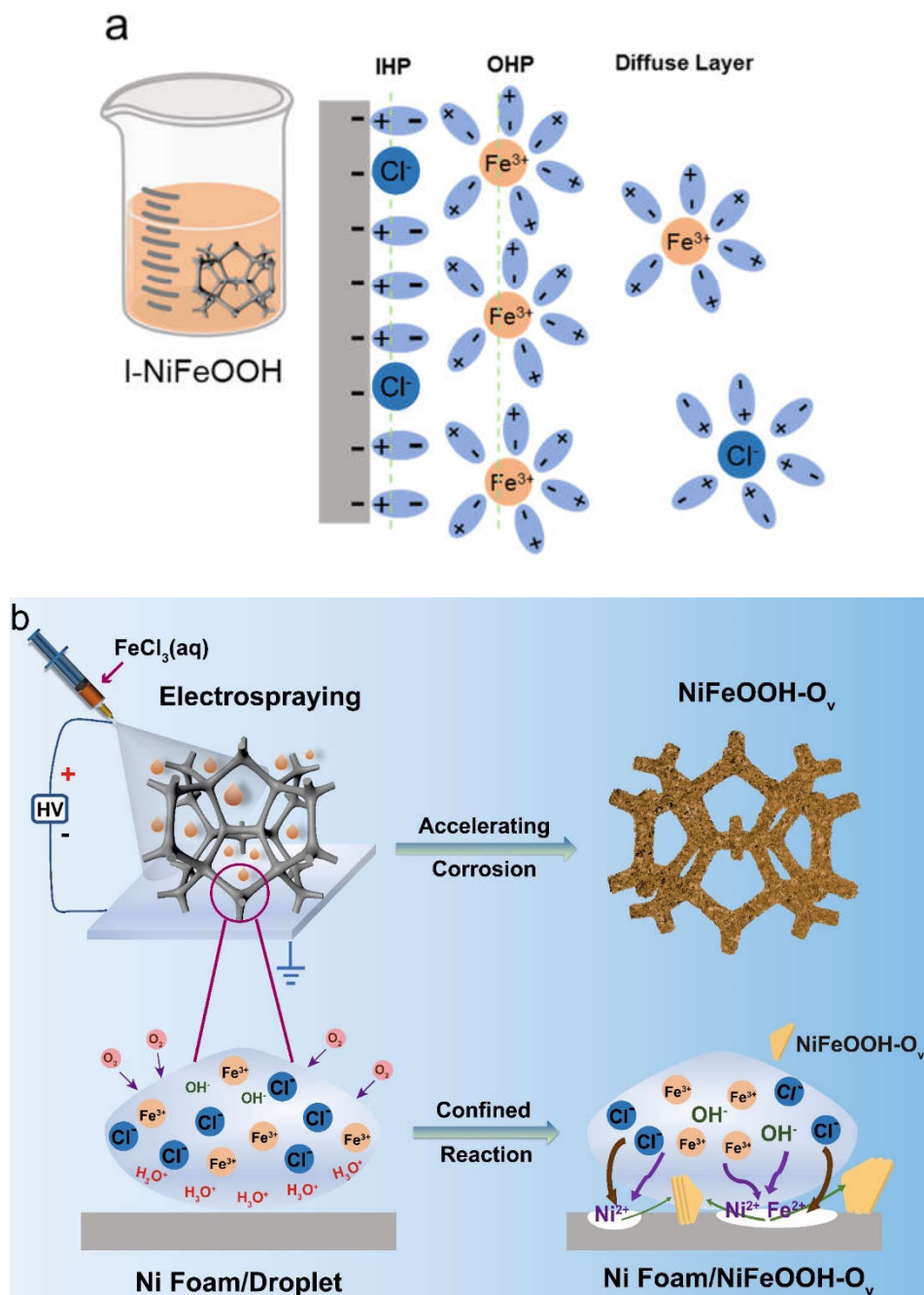


**Figure S1.** a) The corrosion engineering reaction in bulk FeCl<sub>3</sub> aqueous; b) The corrosion engineering reaction mediated by positive charged droplets.

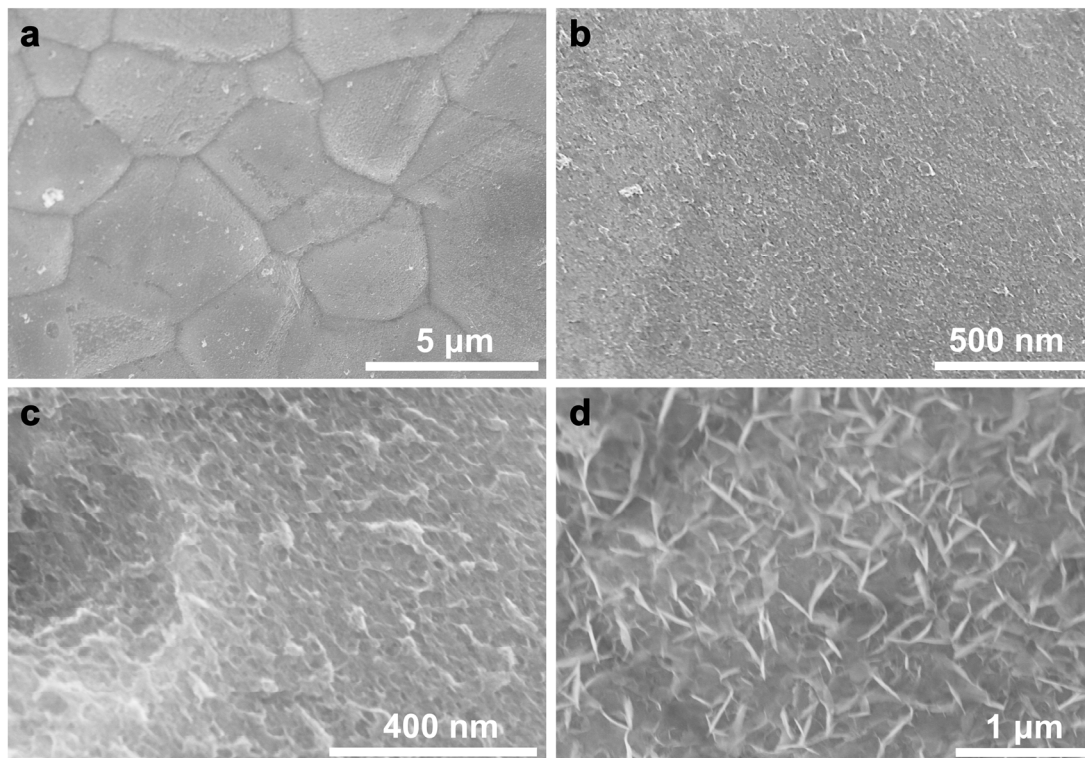


**Figure S2.** a-b) SEM images of the E-NiFeOOH prepared using negative droplets (20 min). c) SEM images of NiFeOOH prepared in the FeCl<sub>3</sub> bulk aqueous (20 min). d) SEM images of E-NiFeOOH prepared using positive droplets (20 min).

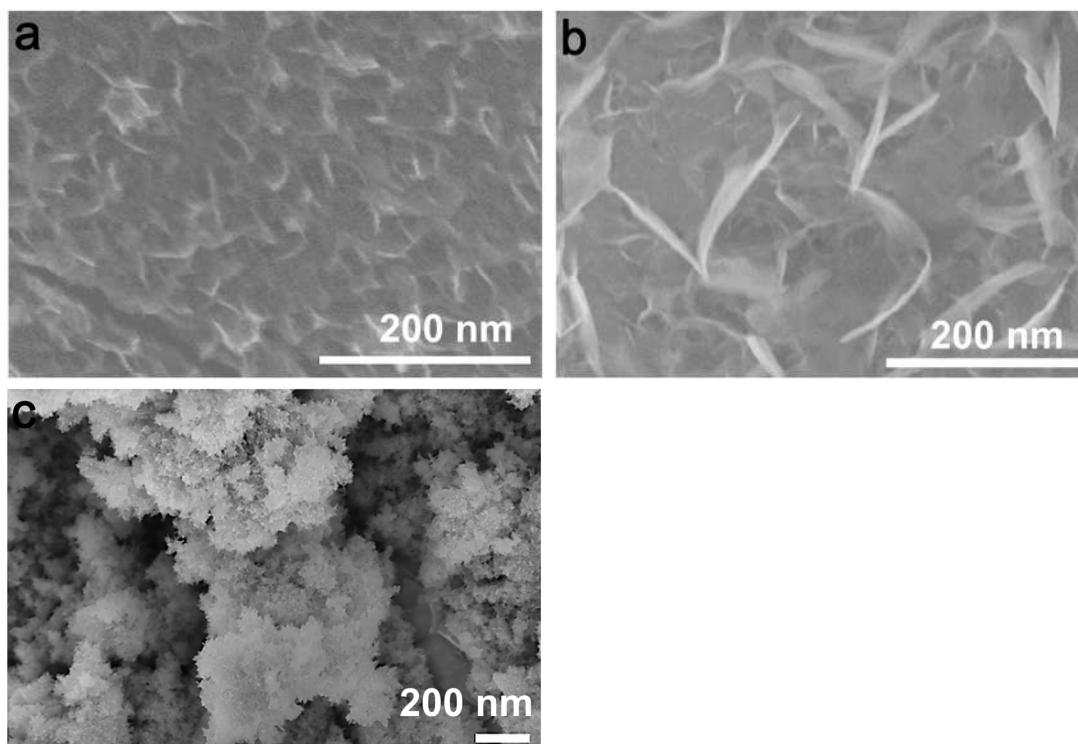


**Figure S3.** SEM images of the E-NiFeOOH with different reaction time (a-10 min, b-20 min and c-60 min).



**Figure S4.** Digital pictures of Ni foam, I-NiFeOOH and E-NiFeOOH with  $1 \times 1 \text{ cm}^2$  area (from left to right).

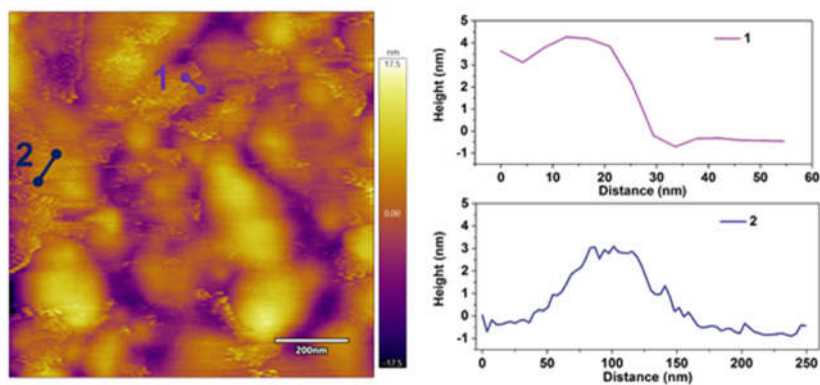


**Figure S5.** AFM image and the corresponding height profiles of E-NiFeOOH nanosheets.

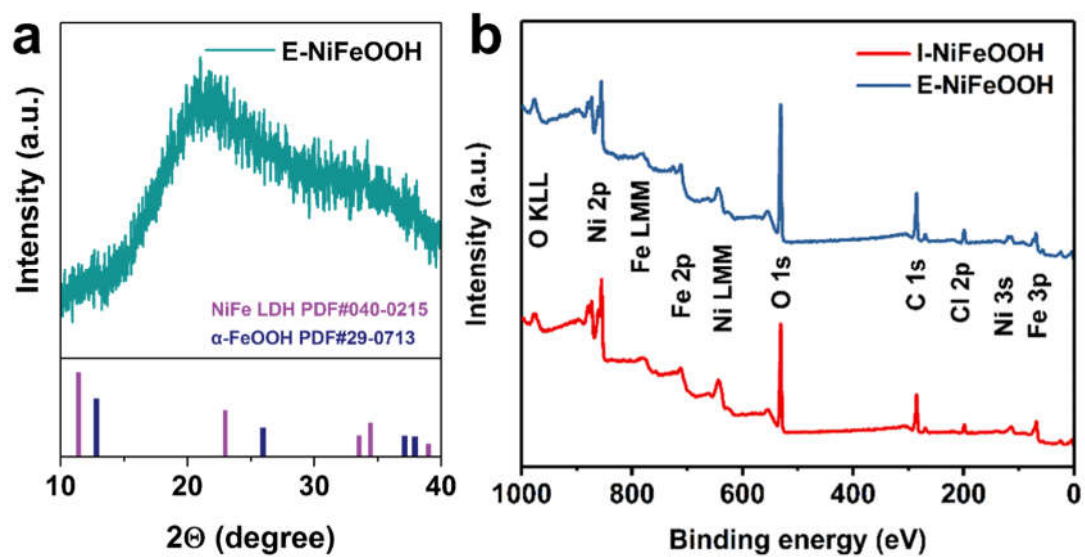


**Figure S6.** a) XRD profiles of E-NiFeOOH. b) XPS survey of I-NiFeOOH and E-NiFeOOH.



Pt/C/NF and E-NiFeOOH at the overpotential of 300 mV. d-e) Polarization curves and corresponding Tafel plots of I-NiFeOOH and E-NiFeOOH for OER. f) Comparison of current density of Ni foam, I-NiFeOOH, RuO<sub>2</sub>/NF and E-NiFeOOH at the overpotential of 300 mV.

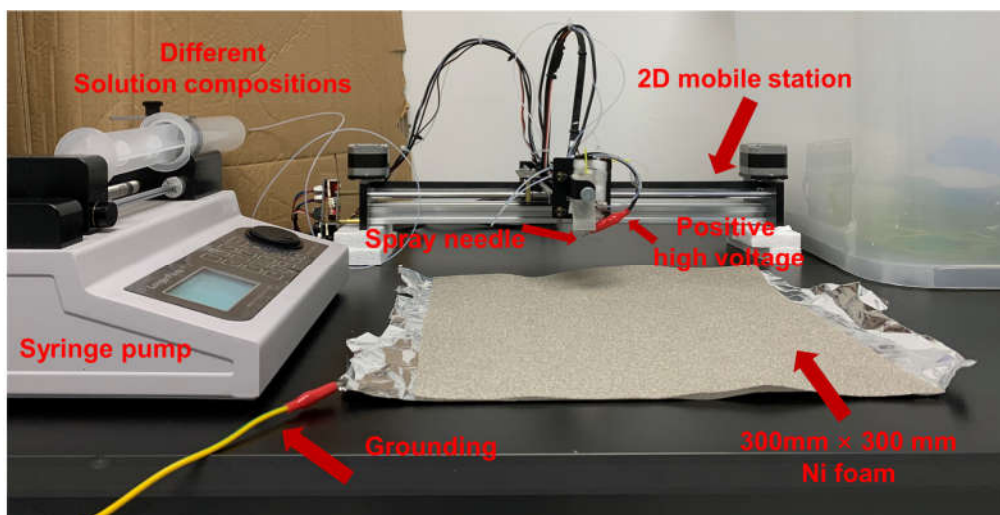


**Figure S9.** The concept scheme of charged droplets mediated corrosion engineering.

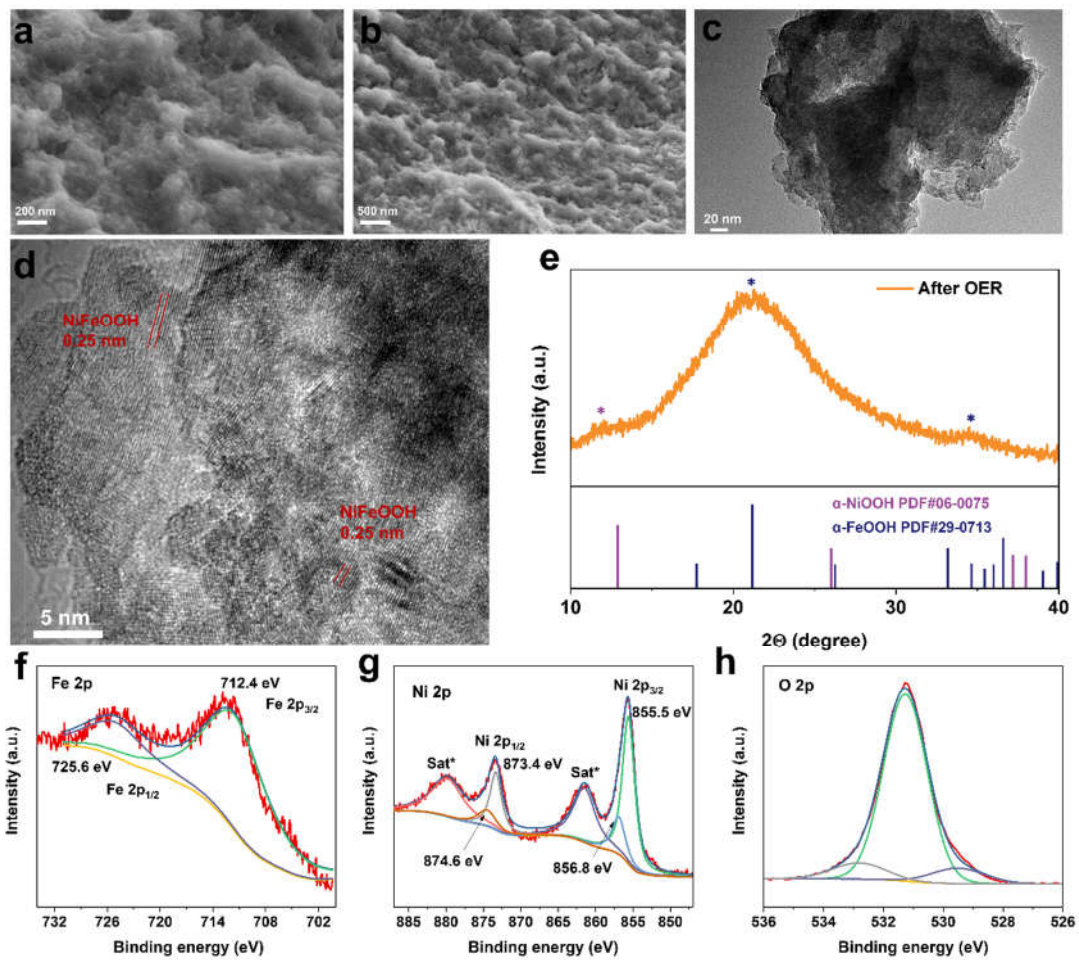


**Figure S10.** The characterization of electrocatalysts after OER reaction a-d) SEM, TEM and HRTEM images, respectively. e-h) XRD spectra and high resolution XPS spectra of Fe 2p, Ni 2p and O 2p, respectively.

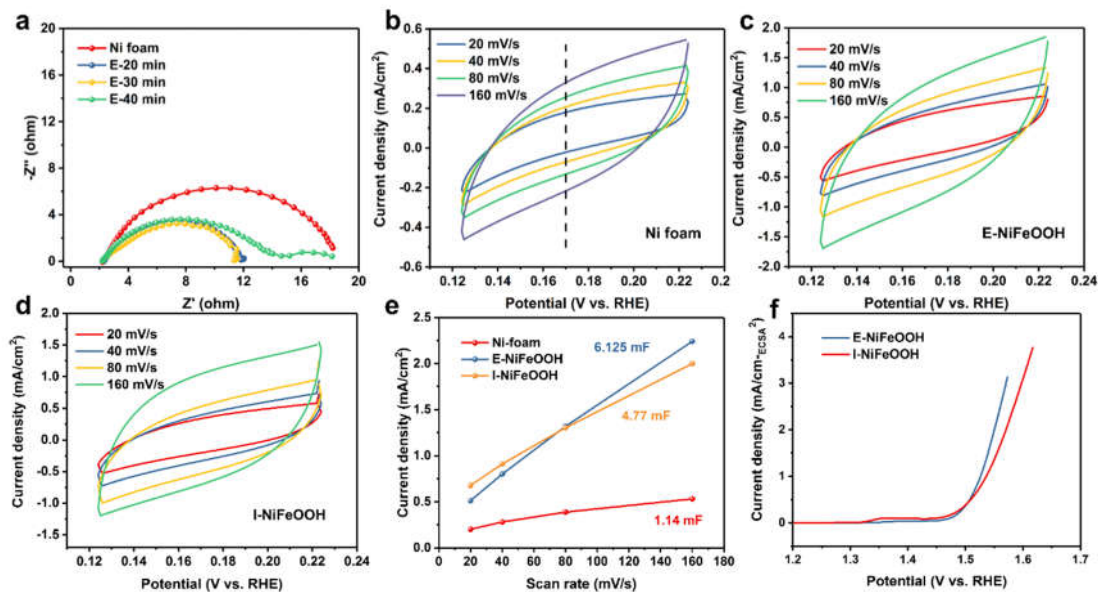


**Figure S11.** a) EIS Nyquist plots of the Ni foam and E-NiFeOOH electrodes prepared using different reaction times in 1 M KOH electrolyte. b-d) Cyclic voltammograms of Ni foam, E-NiFeOOH and I-NiFeOOH with different rates from 20 to 160 mV/s in 1 M KOH electrolyte. e)  $C_{dl}$  values calculated by the capacitive current at 0.17 V (vs. RHE). f) ECSA-normalized LSV curves of I-NiFeOOH and E-NiFeOOH.

**Table S1.** The calculated XPS peak area of M-OH and M-O of I-NiFeOOH and E-NiFeOOH with corresponding estimated  $O_v$  density.

Samples	Oxygen-vacancy Peak Area	M-O Peak Area	$O_v$ density
I-NiFeOOH	59030.02	6479.35	9.11
E-NiFeOOH	84241.48	4329.51	19.46

**Table S2.** Comparison of HER performance of E-NiFeOOH-30 min with other advanced NiFe-based electrocatalysts in 1 M KOH media.

Electrocatalysts	Electrolyte	$\eta_{10}$ (mV)	Tafel slope (mV/dec)	Reference
<b>E-NiFeOOH</b>	<b>1 M KOH</b>	<b>145</b>	<b>115</b>	<b>This work</b>
Porous NiCoFe LTH	1 M KOH	200	70	ACS Energy Lett. 2016, 1, 445
Exfoliated NiFe LDH/defective graphene	1 M KOH	210	110	Adv. Mater. 2017, 29, 1700017-1700024
VOOH hollow nanosphere	1 M KOH	164	104	Angew. Chem., Int. Ed. 2017, 56, 573-577
NiFe LDH	1 M KOH	269	/	Adv. Mater. 2018, 1706279
Ni <sub>2</sub> P	1 M KOH	220	/	Energy Environ. Sci. 2015, 8, 2347.
Ni <sub>3</sub> S <sub>2</sub> NSs/NF	1 M KOH	223	/	J. Am. Chem. Soc. 2015, 137, 14023-14026
Ni/Ni(OH) <sub>2</sub> /Graphite	1 M KOH	225	/	Proc. Natl. Acad. Sci. U.S.A. 2017, 114, 8986–8990.
porous NiFe-oxide nanocubes	1 M KOH	197	130	ACS Appl. Mater. Interfaces 2017, 9, 41906–41915
NiFe LDH@NiCoP/NF	1 M KOH	120	88.2	Adv. Funct. Mater. 2018, 28, 1706847
Ni <sub>12</sub> P <sub>5</sub>	1 M KOH	170	/	ACS Catal. 2017, 7, 103-109
NiCoP/NF	1 M KOH	185	124.4	Adv. Funct. Mater. 2018, 28, 1706847
NiFeOF HF	1 M KOH	253	96	ACS Catal. 2017, 7, 12, 8406–8412
Cu@NiFe LDH	1 M KOH	190	/	Adv. Energy Mater. 2015, 5, 1401660
NiCo <sub>2</sub> S <sub>4</sub> nanowire	1 M KOH	210	58.9	Adv. Funct. Mater. 2016, 26, 4661-4672
NiFe LDH/NF	1 M KOH	210	/	Science 2014, 345, 1593-15960
Ni nanosheets	1 M KOH	130	62	Adv. Mater. 2020, 1906915

**Table S3.** Comparison of OER performance of E-NiFeOOH-40 min with other advanced NiFe-based electrocatalysts in 1 M KOH media.

Electrocatalysts	Electrolyte	$\eta_{10}$ (mV)	Tafel slope (mV/dec)	Reference
<b>E-NiFeOOH</b>	<b>1 M KOH</b>	<b>215</b>	<b>30.7</b>	<b>This work</b>
Ni <sub>2</sub> P@NiFe-LDH	1 M KOH	205	32	Chem. Sci. 2018, 9, 1375.
NiFe-LDH@DG <sub>10</sub>	1 M KOH	210	52	Adv. Mater. 2017, 29, 1700017.
NiFe-LDH-V <sub>Ni</sub>	1 M KOH	229	62.9	Small 2018, 14, 1800136.
NiFe-LDH@graphene	1 M KOH	230	42	ACS Nano 2015, 9, 1977.
Defect NiFe-LDH	1 M KOH	236	39	Adv. Energy Mater. 2019, 9, 1900881.
Fe <sub>6.4</sub> Ni <sub>16.1</sub> P <sub>12.9</sub> B <sub>4.3</sub> O <sub>60.2</sub>	1 M KOH	249	40.3	ACS Nano 2019, 13, 12969.
Fe <sup>2+</sup> -NiFe-LDH	1 M KOH	250	69	Angew. Chem., Int. Ed. 2018, 57, 9392
Atomic layer NiFe-LDH	1 M KOH	254	32	Adv. Energy Mater. 2018, 8, 1703585.
NiFe-LDH/C	1 M KOH	270	56	Angew. Chem. 2017, 129, 11411.
NiFe-LDH	1 M KOH	280	47.6	J. Am. Chem. Soc. 2014, 136, 13118.
Ultra-thin NiFe-LDH	1 M KOH	280	46	Adv. Energy Mater. 2016, 6, 1502585.
NiFe-LDH nanoprisms	1 M KOH	280	49.4	Angew. Chem. 2018, 130, 178.
NiFe-LDH NS	1 M KOH	300	40	Nat. Commun. 2014, 5, 4477.
Porous NiFe oxides	1 M KOH	328	42	Adv. Sci. 2015, 2, 1500199.
R-NiFe CPs	1 M KOH	225	27.78	Adv. Energy Mater. 2020, 2002228
NiFeCr/NF	1 M KOH	270	36	Energy Environ. Sci., 2020

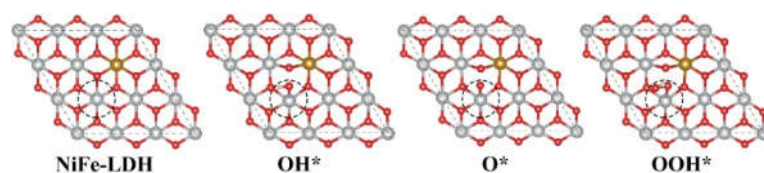
**Table S4.** Comparison of overall water splitting performance of E-NiFeOOH-30 min/E-NiFeOOH-40 min electrodes couple with other advanced NiFe-based electrocatalysts in 1 M KOH media.

Electrocatalysts	Electrolyte	$\eta_{10}$ (V)	Reference
<b>E-NiFeOOH</b>	<b>1 M KOH</b>	<b>1.59</b>	<b>This work</b>
NiFe LDH/Mxene/NF	1 M KOH	1.51	Nano Energy, 2019, 63, 103880
Ni/NiFe LDH	1 M KOH	1.53	J. Mater. Chem. A, 2019, 7, 21722-21729
NiCo <sub>2</sub> S <sub>4</sub> /NF	1 M KOH	1.63	Adv. Funct. Mater. 2016, 26, 4661-4672
Ni <sub>2</sub> P	1 M KOH	1.63	Energy Environ. Sci 2015, 8, 2347-2351
CoP films	1 M KOH	1.63	Angew. Chem. 2015, 127, 6349-6352.
Fe-Ni/NCNTs	1 M KOH	1.64	Angew. Chem., 2018, 57, 8921.
NiFe/NiCo <sub>2</sub> O <sub>4</sub> /NF	1 M KOH	1.67	Adv. Funct. Mater., 2016, 26, 3515-3523
EG/Co <sub>0.85</sub> Se/NiFe-LDH	1 M KOH	1.67	Energy Environ. Sci. 2016, 9, 478-483
CoMnCH/NF	1 M KOH	1.68	J. Am. Chem. Soc., 2017, 139, 8320-8328.
FeCoNi/NCP	1 M KOH	1.687	ACS Catal. 2017, 7, 469-479
PO-Ni/Ni-NCNFs	1 M KOH	1.69	Nano Energy, 2018, 51, 286.
NiFe LDHs/NF	1 M KOH	1.7	Science 2014, 345, 1593-1596
Co(OH) <sub>2</sub> /NCNTs/NF	1 M KOH	1.72	Nano Energy, 2018, 47, 96-104
Ni <sub>3</sub> S <sub>2</sub>	1 M KOH	1.76	J. Am. Chem. Soc. 2015, 137, 14023-14026
NiFe OF	1 M KOH	1.83	ACS Catal. 2017, 7, 12, 8406–8412
Pt/C-IrO <sub>2</sub>	1 M KOH	1.7	Small 2019, 15, 1803639

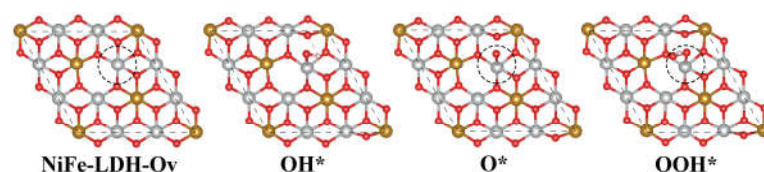
**Table S5.** Calculated total energy  $E$ , zero-point energy  $E_{ZPE}$ , and entropic contribution  $TS$  for all intermediates.

System		$E$ (eV)	$E_{ZPE}$ (eV)	$TS$ (eV)
	*	-161.56	0	0
NiFe-LDH	OH*	-170.20	0.31	0.03
(Ni <sub>9</sub> Fe <sub>1</sub> )	O*	-166.08	0.05	0.06
	OOH*	-174.50	0.43	0.12
	*	-163.33	0	0
NiFe-LDH-O <sub>v</sub>	OH*	-172.43	0.29	0.09
(Ni <sub>3</sub> Fe <sub>1</sub> )	O*	-167.93	0.04	0.10
	OOH*	-176.97	0.41	0.17

**NiFe-LDH(Ni<sub>9</sub>Fe<sub>1</sub>):**



**NiFe-LDH-O<sub>v</sub> (Ni<sub>3</sub>Fe<sub>1</sub>):**



**References**

1. G. Kresse, J. Furthmüller, Phys. Rev. B. 1996, 54, 11169-11186.
2. G. Kresse, J. Hafner, Phys. Rev. B, 1994, 49, 14251-14269.
3. P. E. Blöchl, Phys. Rev. B, 1994, 50, 17953-17979.
4. J. P. Perdew, K. Burke, M. Ernzerhof, Phys. Rev. Lett., 1996, 77, 3865-3868.
5. S. Grimme, J. Comput. Chem. 2006, 27, 1787-1799.
6. A. A. Peterson, F. Abild-Pedersen, F. Studt, J. Rossmeisl, J. K. Nørskov, Energy Environ. Sci., 2010, 3, 1311-1315.